



HAL
open science

Nickel-Catalyzed Trifluoromethylselenolation of Aryl and Alkenyl-Triflates: Scope and Mechanism

Renhe Tang, Julien Petit, Yi Yang, Achim Link, Florian Bächle, Marie-Eve Perrin, Abderrahmane Amgoune, Anis Tlili

► **To cite this version:**

Renhe Tang, Julien Petit, Yi Yang, Achim Link, Florian Bächle, et al.. Nickel-Catalyzed Trifluoromethylselenolation of Aryl and Alkenyl-Triflates: Scope and Mechanism. *ACS Catalysis*, 2023, 13 (19), pp.12553-12562. 10.1021/acscatal.3c02040 . hal-04280420

HAL Id: hal-04280420

<https://hal.science/hal-04280420>

Submitted on 20 Nov 2023

HAL is a multi-disciplinary open access archive for the deposit and dissemination of scientific research documents, whether they are published or not. The documents may come from teaching and research institutions in France or abroad, or from public or private research centers.

L'archive ouverte pluridisciplinaire **HAL**, est destinée au dépôt et à la diffusion de documents scientifiques de niveau recherche, publiés ou non, émanant des établissements d'enseignement et de recherche français ou étrangers, des laboratoires publics ou privés.

Nickel-Catalyzed Trifluoromethylselenolation of Aryl and Alkenyl-Triflates: Scope and Mechanism

Renhe Tang,[†] Julien Petit,^{†,+} Yi Yang,^{†,+} Achim Link,[‡] Florian Bächle,[‡] Marie-Eve L. Perrin,^{,†} Abderrahmane Amgoune,^{*,†,§} and Anis Tlili^{*,†}*

[†]Univ Lyon, CNRS, Université Claude Bernard Lyon 1, ICBMS, UMR 5246, 43 Bd du 11 Novembre 1918, 69622 Villeurbanne (France)

[‡] Solvias AG, Römerpark 2, CH-4303 Kaiseraugst

[§] Institut Universitaire de France (IUF), 1 rue Descartes, 75231 Paris, France

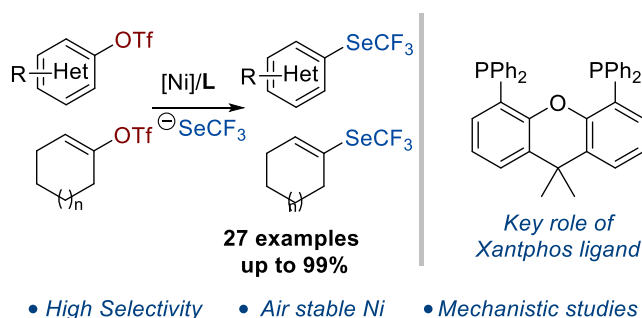
KEYWORDS: Nickel, Cross-Coupling, Trifluoromethylselenolation, Mechanistic Investigation, Xantphos ligand.

ABSTRACT:

The nickel-catalyzed trifluoromethylselenolation of aryl and vinyl triflates is described herein, encompassing synthesis method development and reaction understanding. The challenge lies in the propensity of the Csp^2-SeCF_3 product to undergo reversible oxidative addition to nickel(0) intermediates, potentially initiating catalyst deactivation pathways. In this study, we disclose that Xantphos/Ni(COD)₂ catalytic system is efficient for the synthesis of aryl and vinyl trifluoromethylselenides. The key elementary steps that delineate the catalytic cycles have been investigated by a joint experimental and computational mechanistic investigation and support a Ni⁰/Ni^{II} process. The Xantphos/Ni⁰ system was found to react with both ArOTf and ArSeCF₃ to

give the corresponding (Xantphos)Ni^{II}Ar(X) intermediates (X = OTf or SeCF₃), with the complex (Xantphos)Ni^{II}Ar(OTf) emerging as the most stable. In line with experimental observations, computational studies indicate that oxidative addition of ArSeCF₃ to Xantphos/Ni⁰ is fastest than the oxidative addition of ArOTf but is thermodynamically much less favorable. Thereof, the oxidative addition of ArSeCF₃ is reversible and the product of the ArOTf oxidative addition is yielded as the most stable product. The relative stability of oxidative addition products is attributed to the coordination mode of the Xantphos ligand (κ^2 vs. κ^3) at nickel (II) intermediates. Finally, we demonstrate that ArSeCF₃ compounds can be prepared using an air-stable (Xantphos)Ni(II) pre-catalyst.

TOC graphic:



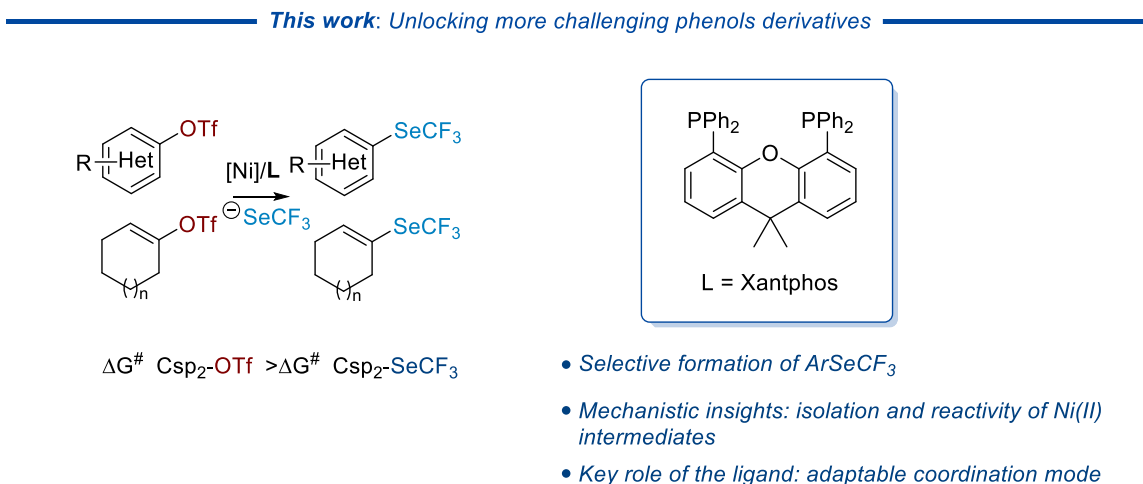
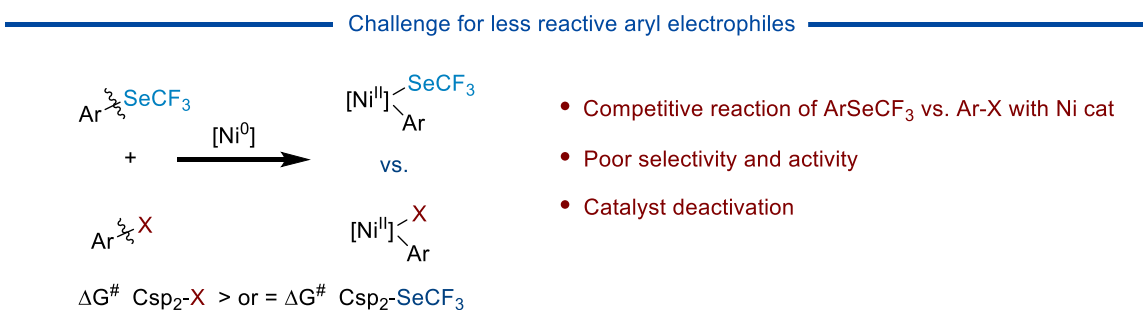
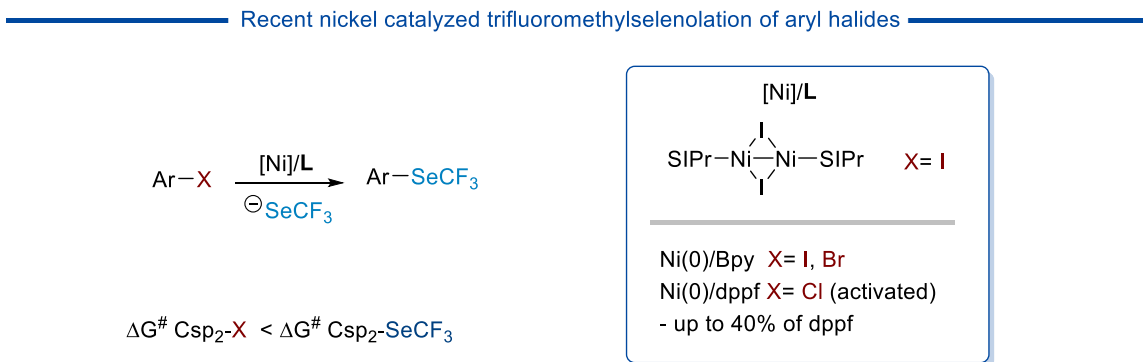
INTRODUCTION

Fluorinated motifs have gained widespread interest and several fluorinated compounds are currently finding applications in life science technology.¹ In this context, the association of chalcogens (O, S and Se) with trifluoromethyl group is covetable due to their interesting physicochemical properties and high lipophilicity.² Though several pharmaceuticals and agrochemicals compounds supporting the OCF₃ motif are commercialized,³ their analogues displaying SCF₃ or SeCF₃ are more scarcely applied.^{1,4} Regarding SeCF₃, attempts to develop

trifluoromethylselenolation reactions through electrophilic, nucleophilic or radical reactions design have been implemented, particularly for the forging of Csp^2 - $SeCF_3$ bonds.⁵ From a retrosynthetic perspective, the trifluoromethylselenolation of aryl halides constitutes an attractive route due to the availability of starting material as well as the potential use of the technology in late-stage functionalization. However, the few methodologies reported mostly involve aryl iodide as starting electrophiles. Additionally, these methodologies rely on the arylation of Me_4NSeCF_3 reagent using either stoichiometric amount of copper under harsh reaction conditions,⁶ or palladium-based catalysis.⁷ More recently, interesting nickel catalyzed trifluoromethylselenolation processes have been reported (Scheme 1). On the one hand, the employment of NHC-Ni(I) dimer proved to be an efficient catalyst for the trifluoromethylselenolation of aryl iodides.⁸ On the other hand, the use of the Ni(0)/Bpy catalytic system revealed its efficiency toward the synthesis of $Ar-SeCF_3$ starting from aryl-iodides or -bromides.^{9,10} Aryl chlorides can also be used as starting electrophiles, but their require the use of Ni(0)/Dppf catalytic loadings up to 40 mol%.⁹ To date, the trifluoromethylselenolation of activated phenol derivatives has not been reported. The main challenge for the development of the trifluoromethylselenolation of Csp^2 -O bonds stands in the inherent reactivity $aryl(Csp^2)-SeCF_3$ towards oxidative addition to nickel(0) species.⁸ Thereof, the trifluoromethylselenolation of aryl electrophiles that are as or less reactive towards Ni(0) than the selenolated awaited product is expected to be intractable.

In this study we report the Ni-catalyzed trifluoromethylselenolation of aryl and vinyl triflates derivatives, under mild conditions. While most of the ancillary ligands provided discouraging results, the use of Xantphos ligand enabled the efficient formation of the desired $ArSeCF_3$ compounds. Mechanistic investigations combining stoichiometric experiments and computational

studies shed light on the key parameters governing the reactivity of XantphosNi(0) species towards the formation of trifluoromethylselenated compounds.



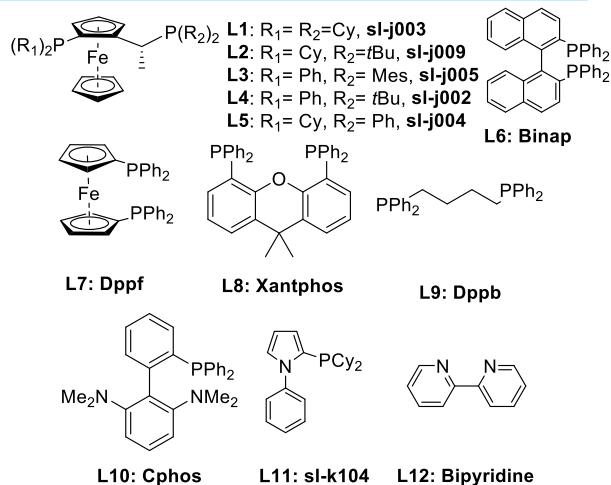
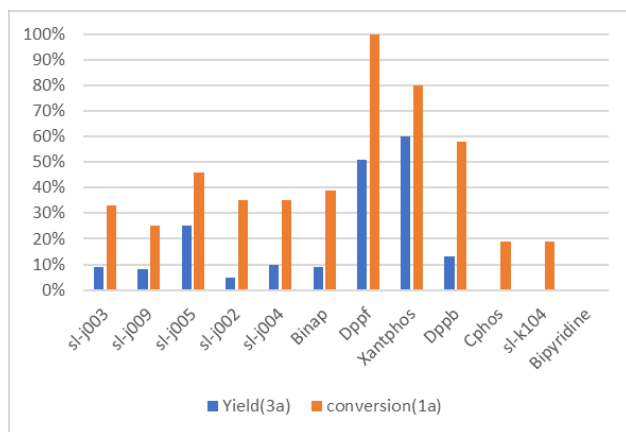
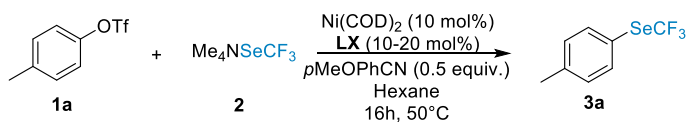
Scheme 1. Current development and challenges for nickel catalyzed trifluoromethylselenolation.

Results and Discussion

Catalyst optimization. The first stage of the investigation began with the identification a ligated Ni complexes that enable the activation of aryl triflates and deliver the desired ArSeCF₃ compounds (Scheme 2). Initial tests were devoted to investigating several Josiphos ligands with different electronic properties in conjunction with Ni(COD)₂. We have previously observed that this ligand platform efficiently sustains Ni(0)/Ni(II) redox pathways, allowing for the nickel-catalyzed selective monoarylation of acetone.¹¹ For preliminary assays, we selected 4-methylphenyltriflate (**1a**) as a model substrate, along with Me₄NSeCF₃ (**2**) as a nucleophile for reactions performed in hexane at 50 °C for 6 h. Importantly, we have used *p*MeOC₆H₄CN as an additive in the aim of generating a more robust and reactive Ni(0) (pre)catalyst.¹²

Under these conditions, Josiphos-type ligands (**L1-L5**) exhibited poor reactivity towards the desired product (Scheme 1). Other diphosphine-ligands such as Binap, Dppf, and Xantphos-type ligands and which have proven efficient in nickel catalyzed cross-coupling reactions of aryl electrophiles including aryl triflates were then screened.¹³ The use of Binap (**L6**) afforded very low amounts of the desired product. Dppf ligand (**L7**) showed 90% conversion of **3a** but with a maximum yield of 50% for the desired product **3a**. This observation contrasts with the reported efficiency of the Dppf/Ni(COD)₂ catalyst for the trifluoromethylthiolation of ArOTf,¹⁴ which points out the enhanced reactivity of ArSeCF₃ vs. ArSCF₃.

Interestingly, the use of Xantphos (**L8**) offered an optimal balance with 80% conversion and 60% yield of the desired product. A low yield of 12% was obtained with Dppb (**L9**), and monophosphines (**L10 & L11**) revealed inefficient as only low conversions were observed without a trace of the desired product. Finally, the use of bipyridine ligand (**L12**), which was recently reported to be an effective ligand for the activation of aryl halides,⁹ was also ineffective for the trifluoromethylselenolation of aryl triflate **1a**.

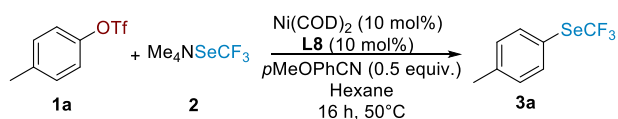


Scheme 2. Ligand screening for the trifluoromethylselenolation of **1a**. [a] Reactions were performed with **1a** (0.1 mmol, 1 equiv.), Ni(COD)_2 (0.01 mmol, 0.1 equiv.), **LX** (0.01 mmol, 0.1 equiv.), **2** (0.15 mmol, 1.5 equiv.), $p\text{MeOC}_6\text{H}_4\text{CN}$ (0.05 mmol, 0.5 equiv.) and solvent (1 mL) for 16 hours. Yields determined by ^{19}F NMR spectroscopy with PhCF_3 as an internal standard. [b] **LX** (0.02 mmol, 0.2 equiv.).

In the second stage, we have investigated other reaction parameters using Xantphos (**L8**) as an optimal ligand. Increasing the reaction temperature to 60°C raised the yield of the desired product **3a** to 78% (Table 1, entry 2). Further increase in the reaction temperature to 70°C proved to be detrimental as **3a** were obtained in 68% yield. Performing the reaction without the nitrile additive ($4\text{-}p\text{MeOC}_6\text{H}_4\text{CN}$) was also detrimental to the reaction outcome, in this case only traces of the desired product were observed (Table 1, entry 4). It is noteworthy that using MeCN as an additive (0.5 equiv.) was not as efficient as $p\text{MeOC}_6\text{H}_4\text{CN}$ for this transformation, as **3a** was obtained only in 6% yield. This suggests that the formation of the reactive $[\text{Ni}(0)\text{-nitrile}]$ adduct is not favorable with acetonitrile (vide infra).¹² In contrast, aromatic nitriles such as PhCN and NaphCN proved to be beneficial for the catalytic activity, although slightly lower yields were obtained than with

*p*MeOC₆H₄CN (Table 1, entries 6 and 7). Performing the reaction in toluene provided the same results as in hexane (Table 1, entry 8), but the combination of hexane and toluene in a 1:1 ratio resulted in the formation of the desired product in 83% yield (entry 9).

Table 1. Optimization of the reaction.^[a]

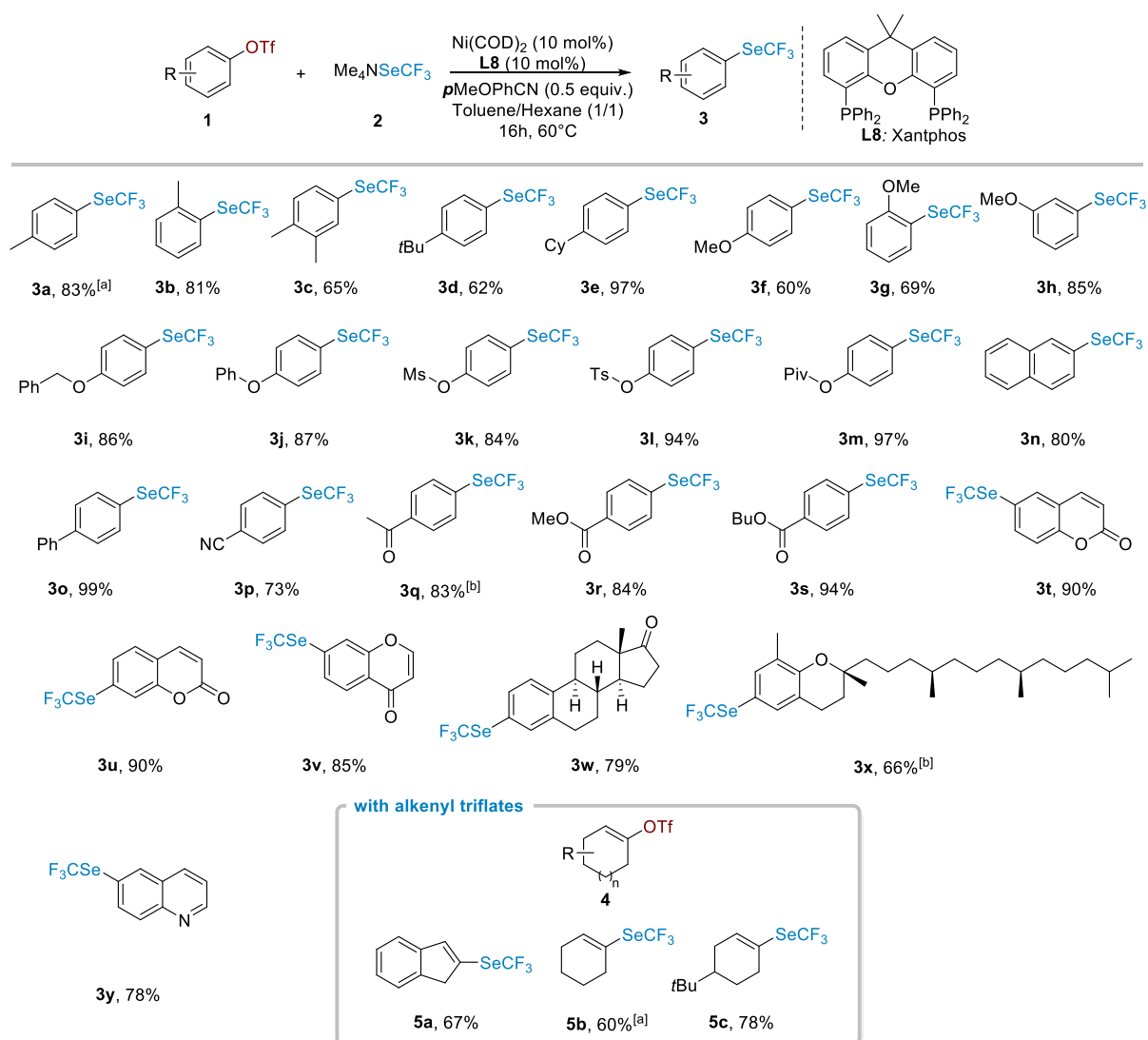


Entry ^[a]	Deviation from standard conditions	Yield ^[b]
1	None	60%
2	60°C instead of 50°C	78%
3	70°C instead of 50°C	68%
4	No <i>p</i> MeOC ₆ H ₄ CN	traces
5	MeCN instead of <i>p</i> MeOC ₆ H ₄ CN	7%
6	PhCN instead of <i>p</i> MeOC ₆ H ₄ CN	68%
7	NaphCN instead of <i>p</i> MeOC ₆ H ₄ CN	66%
8	Toluene	60%
9	Toluene/Hexane (1/1)	83%

[a] Reactions were performed with **1a** (0.1 mmol, 1 equiv.), Ni(COD)₂ (0.01 mmol, 0.1 equiv.), **L8** (0.01 mmol, 0.1 equiv.), **2** (0.15 mmol, 1.5 equiv.), *p*MeOC₆H₄CN (0.05 mmol, 0.5 equiv.) and solvent (1 mL) for 16 hours. [b] Determined by ¹⁹F NMR spectroscopy with PhCF₃ as an internal standard.

Scope of the reaction. With the best reaction conditions in hand, we explored the scope of the reaction. A set of aryl triflates substituted with electron donating groups have been subjected for trifluoromethylselenolation. When the phenyl ring is substituted with a methyl group in *ortho*, *meta* or *para* position, good yields have been obtained ranging from 65% to 83% (Scheme 3, products **3a-3c**). Similarly, when the phenyl ring is substituted with a *t*-butyl or a cyclohexyl group in *para* position, the desired products have been obtained in 62% or 97% yield, respectively

(Scheme 3, products **3d** and **3e**). The reaction also proceeded well with ether substituents (Scheme 3, products **3f-3j**). The presence of other oxygenated leaving groups on the starting aryl triflates have been also investigated. Interestingly, the aryl triflate is selectively and smoothly converted in the presence of mesylate, tosylate as well as pivalate groups with reaction outcomes up to 97% yield (Scheme 3, products **3k-3m**). The naphthene starting material delivered the desired product with 80% yield (Scheme 3, product **3n**). Aryl triflates bearing electron withdrawing groups (Scheme 3, **3o-3s**) were also found to display good reactivity. However, the transformation was shown to be not compatible with carboxylic acids, amido, amino and hydroxyl functional groups, (unsuccessful substrates are provided in SI). The trifluoromethylselenolation of more complex substrates such as coumarin and chromone core structures (Scheme 3, **3t-3v**), an estrone derivative (Scheme 3, **3w**), and a derivative of vitamin E (Scheme 3, **3x**) proceeded with good to very good yields. The exploration of electrophiles was enlarged by considering alkenyl triflate derivatives **4**. Several alkenyl triflates were converted to their corresponding trifluoromethylselenolated analogues in good to very good yields (Scheme 3, products **5a-5c**).



Scheme 3. Substrate scope. [a] Reactions were performed with **1** or **4** (0.2 mmol, 1 equiv.), Ni(COD)₂ (0.02 mmol, 0.1 equiv.), **L8** (0.02 mmol, 0.1 equiv.), **2** (0.3 mmol, 1.5 equiv.), *p*MeOC₆H₄CN (0.1 mmol, 0.5 equiv.) and solvent (1 mL) for 16 hours. Yields of isolated products. [a] Determined by ¹⁹F NMR spectroscopy with PhCF₃ as an internal standard. [b] Ni(COD)₂ (0.03 mmol, 0.15 equiv.), **L7** (0.03 mmol, 0.15 equiv.).

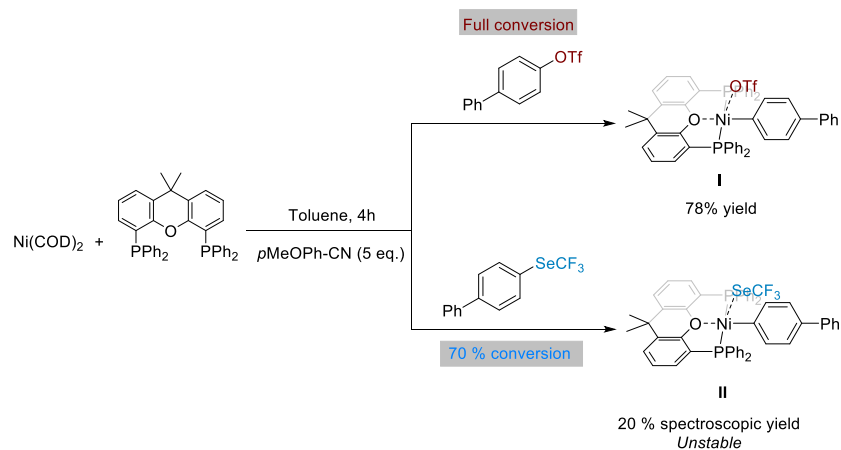
Mechanistic investigations. Having identified optimal conditions for the trifluoromethylselenolation of aryl- and vinyl-triflates, we were eager to collect mechanistic rationale for the observed reactivity of the Xantphos/Ni catalytic system, especially the role played by the nitrile additive and the relative reactivity of the catalysts between the triflate reagent and

the associated trifluoromethylselenolated product. Based on previous mechanistic observations, ArSeCF₃ was anticipated to be more reactive towards the oxidative addition to [Ni(0)] than ArOTf.⁸ However, the trifluoromethylselenolated product can be isolated as the main product and in good yield using the Xantphos/Ni(0) catalytic system. This prompted us to investigate the mechanism of the reaction. More precisely, we were eager to examine the oxidative additions of both ArOTf **1o** and of ArSeCF₃ **3o** to Xantphos-ligated Ni(0) complexes.

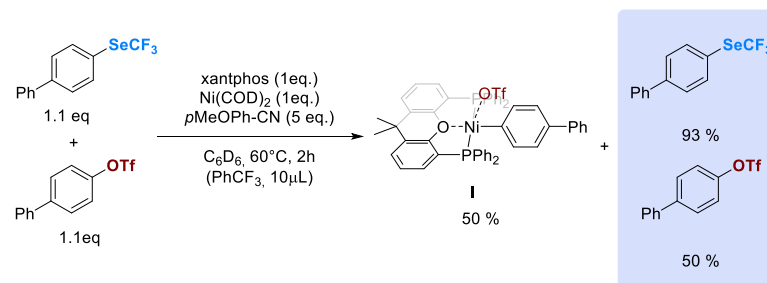
As previously reported, attempts to prepare XantphosNi(COD) by reacting Ni(COD)₂ and 1 equivalent of the Xantphos ligand **L8** in toluene resulted in the precipitation of (Xantphos)₂Ni as the major species.¹⁵ This complex has poor solubility in most solvents, but its formation was confirmed by X-Ray diffraction analysis (See ESI for details).¹⁶ This species is not reactive under our catalytic conditions (see Table 1, entry 4). Additionally, when Ni(COD)₂ and 1 equivalent of Xantphos were reacted in the presence of aryl triflate **1o**, only precipitation of (Xantphos)₂Ni was observed, no oxidative addition product was detected. The beneficial effect of the nitrile additive, as observed during catalysis, was found to arise from the ability of the nitrile to displace one Xantphos ligand and form a catalytically active (Xantphos)Ni(nitrile) complex.¹⁵ We have experimentally confirmed that the addition of 5 to 10 equivalents of *p*-methoxybenzotrile to the reaction mixture led to an equilibrium between (Xantphos)₂Ni and the nitrile adduct (Xantphos)Ni(*p*MeOC₆H₄CN) that is formed up to 34%. Notably, it was found that acetonitrile is not efficient in forming the (Xantphos)Ni(MeCN) complex, which explains the poor catalytic activity observed in the presence of acetonitrile (Table 1, entry 5).¹⁷ Then, the oxidative addition of *p*-phenyl-phenyltriflate **1o** to Ni(0) complexes yielded from Xantphos and Ni(COD)₂ in the presence of 5 eq. of *p*-methoxybenzotrile has been investigated. The reaction proceeded at room temperature and resulted in the rapid formation of the oxidative addition complex **I**, which was

isolated in 78% yield (Scheme 4A). The formation of complex **I** was confirmed in solution by NMR spectroscopy. The $^{31}\text{P}\{^1\text{H}\}$ NMR spectrum of complex **I** displayed a single resonance signal at $\delta = 11.4$ ppm indicating a *trans*-symmetric coordination of both phosphorus atoms.¹⁸ In addition, the ^{19}F NMR resonance signal of the triflate moiety is shifted to $\delta = -78.8$ ppm, suggesting a weak coordination to the Ni center. ESI mass spectrometry analyses of **I** clearly indicated the formation of a cationic (Xantphos)nickel(II) aryl species (mass peak at 789.1981 m/z for $[\text{C}_{51}\text{H}_{41}\text{OP}_2\text{Ni}^+]$). Unfortunately, all attempts to characterize the corresponding complex by X-ray diffraction analysis were unsuccessful. The characterization data of complex **I** indicates the formation of a square planar nickel complex with a weakly coordinated OTf counter anion.¹⁹

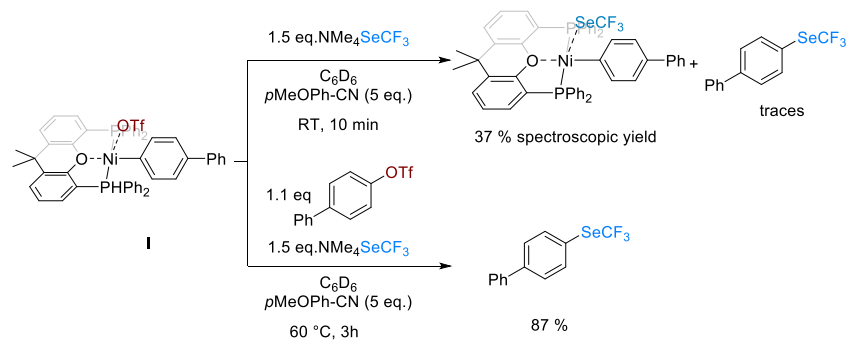
A. Oxidative addition of Ar-OTf and Ar-SeCF₃ to Xantphos(Ni)⁰



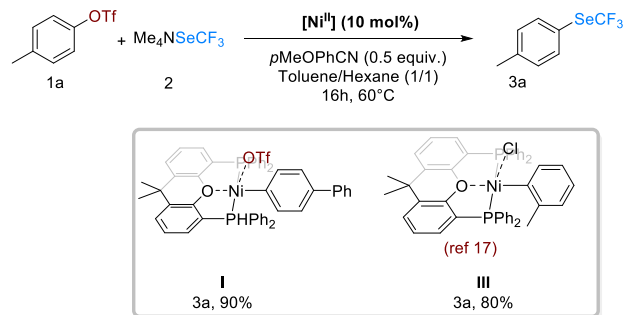
B. Competitive oxidative addition of ArOTf vs. Ar-SeCF₃ to Xantphos(Ni)⁰



C. Stoichiometric reaction of complex I with NMe₄SeCF₃



D. Catalytic activity of XantphosNi(II) complexes



Scheme 4. Mechanistic investigations: A, B. Comparative reactivity of Xantphos/Ni(COD)₂/p-methoxybenzonitrile with ArOTf **1o** and ArSeCF₃ **3o**. C. trifluoromethylselenolation of ArOTf using complex **I**. D. Catalytic reactivity of XantphosNi(II) complexes. Yields of complexes were determined by ³¹P NMR and product yields by ¹⁹F NMR spectroscopy with PhCF₃ as an internal standard.

Then, we investigated the reactivity of *p*-phenyl-phenylSeCF₃ **3o** towards oxidative addition to XantphosNi(0) in presence of nitrile was investigated. In this case, monitoring the reaction by ¹⁹F NMR spectroscopy revealed significant consumption of **3o** (70 % conversion) after 4h at room temperature in C₆D₆, along with the formation of a single species appearing as a singlet at $\delta = -17$ ppm with an overall spectroscopic yield of 20%. The ¹⁹F NMR chemical shift of the new species falls within the same region as trifluoromethylselenate metal complexes previously described.²⁰ Additionally, the new species displays a ³¹P NMR resonance signal at $\delta = 7.5$ ppm, very close to that observed for complex **I**. These NMR data suggest that XantphosNi(0) also readily undergoes oxidative addition of ArSeCF₃ to give the corresponding (Xantphos)Ni(II)(Ar)(SeCF₃) species (Scheme 4B). The NiSeCF₃ intermediate was found to be unstable, as it gradually disappears over time or upon heating to 60°C, while ArSeCF₃ is further consumed. Unfortunately, all attempts to isolate and further characterize the NiSeCF₃ intermediate and its degradation product(s) were unsuccessful. After 20 hours of reaction the ¹⁹F NMR spectrum of the reaction mixture showed only two minor resonance signals corresponding to residual ArSeCF₃ reactant **3o** (8%) and to PhSeCF₃ (30%).²¹ The reaction of Xantphos/Ni(0) species with aryl halides has been previously shown to lead to the formation of Ni(I) intermediates concomitantly with high amount of bi-aryl compounds.²² Such a pathway may also be operative for ArSeCF₃ to explain the decomposition process; however, no traces of bi-aryl compounds could be detected. These observations along with previous reports indicating that DppfNi(I) species are ineffective as catalyst for the formation of C-SCF₃ bonds^{14,23} suggest that the formation of Ni(I) species in catalytic conditions is not predominant.

Overall, these observations indicate that both ArOTf and ArSeCF₃ can react readily with XantphosNi(0) species at room temperature. Remarkably, when the reaction is performed in the

presence of stoichiometric amount of both substrates, only the triflate derivative is converted towards the formation of the corresponding nickel(II) aryl species **I** (50% ^{19}F NMR spectroscopic yield). Under the same conditions, the ArSeCF_3 substrate remained almost intact. To further confirm the formation of a NiSeCF_3 intermediate, a stoichiometric reaction between complex **I** and $\text{NMe}_4\text{SeCF}_3$ was carried out. Within 10 minutes at room temperature, ^{19}F and ^{31}P NMR spectroscopic analyses of the reaction mixture indicated the formation of complex **II** (37 % ^{31}P NMR spectroscopic yield) along with traces of the ArSeCF_3 coupling product. Upon further heating the reaction to 60°C for several hours, the signals associated with complexes **I** and **II** disappeared, with only a slight increase in the coupling product. However, when the reaction is carried out in the presence of one equivalent of ArOTf **10**, the formation of the desired product **30** is observed in high yield (87% yield, Scheme 4). These observations suggest that salt metathesis is operative to give a selenated nickel intermediate **II**. The C-SeCF_3 reductive elimination from complex **II** would proceed with an equilibrium constant favoring the reverse oxidative addition. Under stoichiometric conditions, the addition of ArOTf is necessary to shift the equilibrium toward the formation of thermodynamically stable complex **I** and the release of the desired product. The catalytic efficiency of complex **I** was further confirmed, providing the trifluoromethylselenated product in high yields. Notably, similar results were obtained using previously reported XantphosNi(II) aryl chloride analogue complex **III**.²⁴

All together, these results support a Ni(0)/Ni(II) pathway, which is initiated by the oxidative addition of ArOTf to a mono-Xantphos-ligated Ni(0) complex, followed by salt metathesis and subsequent reductive elimination.

To complement the experimental mechanistic investigation, a computational study was conducted at the M06/CPCM(PhMe)/def2-TZVP:SDD-ECP//B3PW91/6-311G(2d,p):LANL2-

ECP DFT level (see ESI for computational details) to confirm the key intermediates and to assess the energetics of the most relevant reaction steps. Xantphos ligand was modeled without structural simplification, and PhOTf was used as a typical electrophile. Unless specified ionic species were considered separated from their counter ion. The (Xantphos)Ni(nitrile) adduct **A** was optimized as a minimum on the potential energy surface. Its formation is computed endergonic by only 7.8 kcal mol⁻¹ relative to separated (Xantphos)₂Ni, Ni(COD)₂ and nitrile (Figure 1). This result is consistent with detailed experimental mechanistic observations and previous reports,^{12,15} but also with the equilibrium in solution of (Xantphos)₂Ni, Ni(COD)₂ and complex **A** as previously discussed.

The oxidative addition of PhOTf to complex **A** requires overcoming a Gibbs energy barrier of 16.8 kcal.mol⁻¹ to yield the nickel(II) aryl complex **B** whose formation is computed exergonic by 19.4 kcal.mol⁻¹ relative to **A** and the associated reactants. In comparison, the oxidative addition of PhSeCF₃ to complex **A** is much faster, as indicated by a computed Gibbs energy barrier of 11.4 kcal.mol⁻¹. This is consistent with the observed experimental reactivity trend and in line with the computed (Ar)C-SeCF₃ bond dissociation energies that is weaker than the (Ar)C-OTf one by 21 kcal mol⁻¹ (See ESI). Thermodynamically, formation of the resulting (Xantphos)Ni^{II}(Ph) (SeCF₃) complex in its singlet (**C**) or triplet state (**D**) is exergonic by ca. 4 kcal mol⁻¹, which is less stable by ca. 15 kcal.mol⁻¹ than the PhOTf oxidative addition product. Therefore, it is likely that the (Xantphos)Ni^{II}(Ph)(SeCF₃) (**C**) intermediate is formed but undergoes rapid reductive elimination ($\Delta G^\ddagger = 15.4$ kcal mol⁻¹) to regenerate the Ni(0) adduct **A**, which ultimately performs the oxidative addition of the triflate with an overall Gibbs energy barrier of 20.8 kcal.mol⁻¹ and a global exergonicity of 15.4 kcal.mol⁻¹. This mechanistic picture is consistent with the experimental observation.

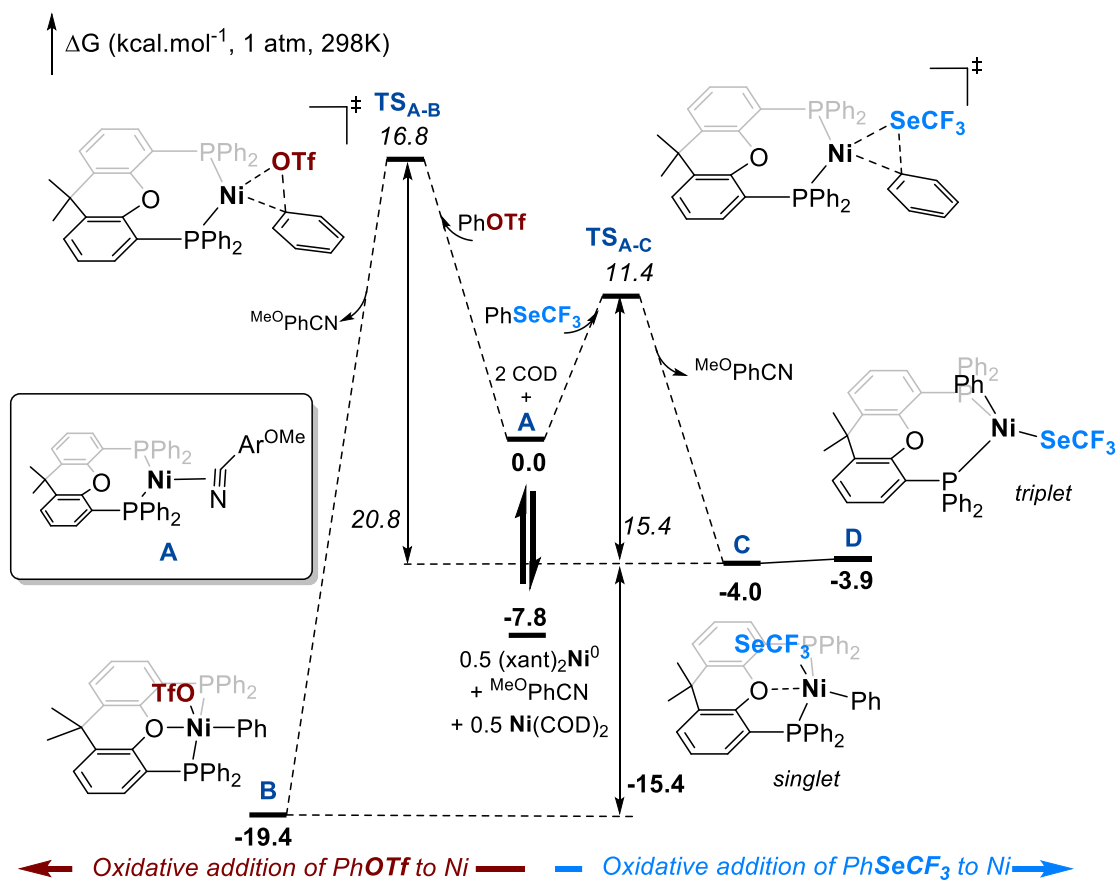


Figure 1. Simplified Gibbs energy profile for the oxidative addition of PhOTf vs. PhSeCF₃ (see level of theory in ESI).

For comparative analysis, we have conducted the same computational investigation using Dppf as a bidentate ligand (see ESI for details). Starting from the (Dppf)Ni(nitrile) adduct, the computed Gibbs energy barriers for the oxidative addition of PhOTf and PhSeCF₃ stand at 14.4 and 10.6 kcal.mol⁻¹, respectively. Both processes were also found to be thermodynamically favorable, by 13.8 kcal.mol⁻¹ for (Dppf)Ni^{II}(Ph)(SeCF₃) and by 21.2 kcal.mol⁻¹ for (Dppf)Ni^{II}(Ph)(Otf).

Analogously to that observed with Xantphos ligand, these results indicate that both reactions are feasible and the kinetic preference for PhSeCF₃ oxidative addition. The resulting oxidative addition

intermediates are thermodynamically stable, with $(\text{Dppf})\text{Ni}^{\text{II}}(\text{Ph})(\text{SeCF}_3)$ being more stable than the corresponding $(\text{Xantphos})\text{Ni}^{\text{II}}(\text{Ph})(\text{SeCF}_3)$ intermediate.

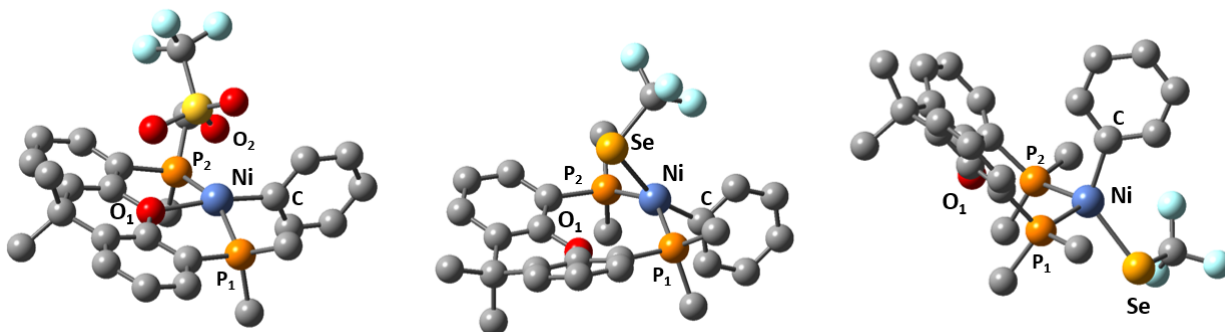
It is worth noting that the oxidative addition of ArSCF_3 to $(\text{Dppf})\text{Ni}(0)$ species was reported to lead to a catalytically inactive species.¹⁴ This insight raises the possibility that the computed $(\text{Dppf})\text{Ni}(\text{II})\text{SeCF}_3$ intermediate may undergo decomposition rather than reversible reductive elimination. Additionally, the oxidative addition of ArOTf to $(\text{Dppf})\text{Ni}(0)$ species may lead to $(\text{DPPF})\text{Ni}(\text{I})$ species, via a subsequent comproportionation pathway.²³ These species have been shown to lead to inactive species in the context of trifluoromethylthiolation of aryl halides.²³

Thus, on one hand the thermodynamic stability of $(\text{Xantphos})\text{Ni}^{\text{II}}(\text{Ph})(\text{OTf})$ may prevent from the competitive formation of $\text{Ni}(\text{I})$ species. On the other hand, the comparatively diminished stability of $(\text{Xantphos})\text{Ni}^{\text{II}}(\text{Ph})(\text{SeCF}_3)$ enables facile reverse reductive elimination and thus do not eventually lead to catalytically inactive species.

To get more insights into the factors that account for the important difference of thermodynamic stability between $(\text{Xantphos})\text{Ni}^{\text{II}}(\text{Ph})(\text{OTf})$ and $(\text{Xantphos})\text{Ni}^{\text{II}}(\text{Ph})(\text{SeCF}_3)$ intermediates, optimized structures of $\text{XantphosNi}(\text{II})$ complexes **B** and **C** were analyzed. In complex **B**, the nickel center exhibits a square pyramidal geometry in which the tridentate $\kappa^3\text{-P,O,P}$ Xantphos ligand and the phenyl ring form the base of the pyramid, while the OTf ligand occupies the apical position. The distance between the OTf anion and the metal center is relatively short (2.321 Å), much shorter than the sum of the van der Waals radii of Ni and O atoms (3.15 Å). The deviation of Ni from the base is only around 0.28 Å relative to an ideal square-based pyramid geometry, indicating a slightly distorted geometry. In contrast, complexes $(\text{Xantphos})\text{Ni}^{\text{II}}(\text{Ph})(\text{SeCF}_3)$ (**C** or **D**) display tetrahedral geometries in which the Xantphos ligand is no longer tridentate but $\kappa^2\text{-P,P}$

bidentate as illustrated in Table 2. The optimized Ni-Se distances of 2.44 Å in **C** and 2.40 Å in **D** are short relative to the sum of the Ni and Se van der Waals radii (3.53 Å), potentially indicating a strong interaction.

Table 2. Top: From left to right: computed structures of complexes **B**, **C** and **D**. Bottom: angles and distances of computed structures.



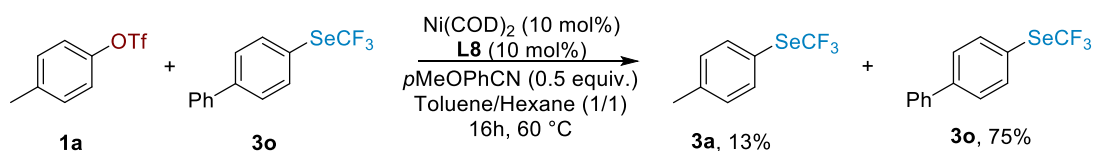
	Distance (Å)				Angles (°)			
	Ni-O ₁	Ni-O ₂	Ni-Se	Ni-C	P ₁ -Ni-P ₂	O ₁ -Ni-C	C-Ni-Se	O ₂ -Ni-C
B	2.100	2.321	-	1.872	154.9	172.5	-	101.9
C	2.755	-	2.449	1.888	142.9	120.7	160.7	-
D	3.456	-	2.409	1.972	107.2	92.5	123.0	-

The weaker coordination of the OTf moiety to Ni compared to SeCF₃, induces a different coordination mode of the Xantphos ligand, which significantly impacts the coordination geometry around the nickel(II) center.

Overall, this computational mechanistic study suggests that the formation of compound **C** is kinetically favored, yet reversible, while formation of compound **B** is thermodynamically favored. Consequently, the activation of PhSeCF₃ is unlikely to significantly disturb the catalytic trifluoromethylselenolation of PhOTf under the experimental conditions used. The important Gibbs free energy difference observed between compound **C** and compound **B** ($\Delta G = 15.4$

kcal.mol⁻¹) may originate from the different coordination geometry around the nickel(II) center induced by the Xantphos ligand (κ^3 -P,O,P vs. κ^2 -P,P). This may explain the superior catalytic efficiency of Xantphos compared to other bidentate ligands.²⁵

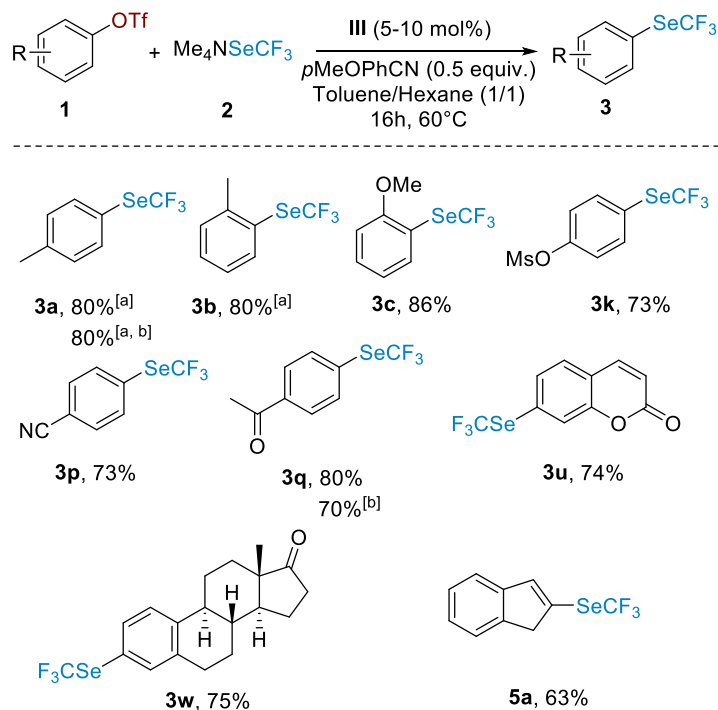
Finally, to further confirm that oxidative addition of ArSeCF₃ occurs during catalysis, we hypothesized that trifluoromethylselenolation of Ar²OTf may be observed using one equivalent of Ar¹SeCF₃ as the -SeCF₃ precursor. This process would entail the concomitant oxidative addition of both Ar¹SeCF₃ and Ar²OTf substrates, followed by ligand exchange and reductive elimination to give some Ar²SeCF₃ product. To test this hypothesis, we conducted a catalytic reaction using a 1/1 ratio of 4-MePhOTf **1a** and 4-PhPhSeCF₃ **3o** under identical reaction conditions. We were delighted to observe the formation of the desired product **3a** 4-MePhSeCF₃ albeit in low yield of 13% and recovering of 75% of the starting **3o** (Scheme 5). This experiment evidences the occurrence of some ArSeCF₃ oxidative addition during catalysis.



Scheme 5. trifluoromethylselenolation of ArOTf **1a** using **3o** as SeCF₃ precursor.

Finally, we sought to evaluate the use of Ni(II) precatalysts instead of air sensitive Nickel(0) precursors. While the combination of Xantphos with nickel(II) salts in the presence of reductants (Zn, Mn or TDAE) is not operative for this transformation (see ESI for details), we found that the isolated (Xantphos)Ni(II)(OTf)PhPh complex **II** was very efficient for the trifluoromethylselenolation of **1a** affording the desired product in 90% yield. However, as complex

II was found to be air sensitive, our attention turned to complex **III** that is air stable. Using **III**, the trifluoromethylselenolation of aryl and vinyl triflates were explored. To our delight, complex **III** performs well the trifluoromethylselenolation independently of the stereo-electronic features of the electrophile substituents, encompassing more complex structures (Scheme 6). Interestingly, starting with **III** enabled us to decrease the catalyst loading down to 5 mol% with similar reaction outcome (compound **3a**, or **3q** Scheme 6). Notably, we also observed interesting reactivity with alkenyl triflates, and were able to obtain compound **5a** with a yield of 63% (Scheme 6).



Scheme 6. Substrate scope with complex **III** [a] Reactions were performed with **1** or **4** (0.2 mmol, 1 equiv.), **III** (0.02 mmol, 0.1 equiv.), **2** (0.3 mmol, 1.5 equiv.), $p\text{MeOC}_6\text{H}_4\text{CN}$ (0.1 mmol, 0.5 equiv.) and solvent (1 mL) for 16 hours. Yields of isolated products. [a] Determined by ^{19}F NMR spectroscopy with PhCF_3 as an internal standard. [b] **III** (0.01, 0.05 equiv.)

Conclusion

In this study, we have presented the first example of a nickel-catalyzed trifluoromethylselenolation of C-O bonds, which is efficient for both electron donating and electron withdrawing substituted aryl triflates as well as more complex structures and alkenyl triflates. By conducting detailed mechanistic studies, combining experimental and computational investigations, we have been able to elucidate the feasibility and selectivity of each key elementary step involved in the catalytic cycle. Our investigations revealed that the XantphosNi(0) precursors are able to activate both Csp²-OTf and Csp²-SeCF₃ bonds, giving rise to the corresponding nickel(II) intermediates that have been spectroscopically assessed. However, only the (Xantphos)Ni(II)(Ar)(OTf) intermediate is thermodynamically stable, providing a driving force for the desired transformation. The ability of Xantphos ligand to accommodate different coordination modes was found to be at the origin of the different stability between Ni(II)-OTf and Ni(II)-SeCF₃ intermediates. Additionally, we have demonstrated that the reversibility of the Csp²-SeCF₃ bond activation at XantphosNi(0) species open very promising opportunities to develop new synthetic pathways towards the formation of SeCF₃-product.

AUTHOR INFORMATION

Corresponding Author

marie-eve.perrin@univ-lyon1.fr

abderrahmane.amgoune@univ-lyon1.fr

anis.tlili@univ-lyon1.fr

The manuscript was written through contributions of all authors. All authors have given approval to the final version of the manuscript.

[†]These authors contributed equally.

ASSOCIATED CONTENT

Supporting Information.

Experimental procedures, spectral and analytical data including NMR spectra (PDF)

Crystallographic data for [(Xantphos)₂Ni] complex (CIF)

ACKNOWLEDGMENT

Financial support from the CNRS and the University Lyon 1 are gratefully acknowledged. R.T and Y.Y thanks the CSC (China Scholarship Council) for a doctoral fellowship. A.A. thanks the Institut Universitaire de France (IUF) for its support. The NMR (CCRMN) and Mass (CCMS) Centers of the Université Claude Bernard Lyon 1 are gratefully acknowledged for their contribution. Erwann Jeanneau from the Centre de Diffractométrie Henri Longchambon, Université Lyon 1 is acknowledged for the X-ray diffraction analysis of [(Xantphos)₂Ni] complex. The CCIR of ICBMS is acknowledged for a generous allocation of computational resources and providing technical support. We thank abcr for providing Me₄NF.

REFERENCES

¹ (a) Kirsch, P. in *Modern Fluoroorganic Chemistry*, Wiley-VCH, *Weinheim*, **2013**. (b) Ogawa, Y.; Tokunaga, E.; Kobayashi, O.; Hirai K.; Shibata, N. Current contributions of organofluorine compounds to the agrochemical industry. *iScience*. **2020**, *23*, 101467. (c) Inoue, M.; Sumii, Y.; Shibata, N. Contribution of organofluorine compounds to pharmaceuticals. *ACS Omega* **2020**, *5*, 10633–10640.

² (a) Ge, H.; Liu, H.; Shen, Q. in *Organofluorine Chemistry* **2021**, 99–172. (b) Ghiazza, C.; Tlili, A. Copper-promoted/copper-catalyzed trifluoromethylselenolation reactions. *Beilstein, J. Org. Chem.* **2020**, *16*, 305-316. (c) Xu, X.-H.; Matsuzaki K.; Shibata, N. Synthetic methods for

compounds having CF₃-S units on carbon by trifluoromethylation, trifluoromethylthiolation, triflylation, and related reactions. *Chem. Rev.* **2015**, *115*, 731–764. (d) Besset, T.; Jubault, P.; Pannecoucke, X.; Poisson, T. New entries toward the synthesis of OCF₃-containing molecules. *Org. Chem. Front.*, **2016**, *3*, 1004–1010.

³ Liu, J.; Lin, W.; Sorochinsky, A. E.; Bulter, G.; Landa, A.; Han, J.; Soloshonok, V. A. Successful trifluoromethoxy-containing pharmaceuticals and agrochemicals. *J. Fluorine Chem.* **2022**, *257-258*, 109978

⁴ Ghiazza, C.; Billard, T.; Dickson, C.; Tlili, A.; Gampe, C. M. Chalcogen OCF₃ isosteres modulate drug properties without introducing inherent liabilities *ChemMedChem*, **2019**, *17*, 1586-1589.

⁵ (a) Tlili, A.; Ismalaj, E.; Glenadel, Q.; Ghiazza, C.; Billard, T. Synthetic approaches to trifluoromethylselenolated compounds. *Chem. Eur. J.* **2018**, *24*, 3659-3670. (b) Ghiazza, C.; Billard, T.; Tlili, A. Merging visible-light catalysis for the direct late-stage group 16-trifluoromethyl bond formation. *Chem. Eur. J.*, **2019**, *25*, 6482-6495. (c) Louvel, D.; Ghiazza, C.; Debrauwer, V.; Khrouz, L.; Monnereau, C.; Tlili, A. Forging C-SeCF₃ bonds with trifluoromethyl tolueneselenosulfonate under visible-light. *Chem. Rec.* **2021**, *21*, 417-426. For the use of diazonium salts for trifluoromethylselenolation see: (d) Matheis, C.; Wagner, V.; Goossen, L. J. Sandmeyer-Type Trifluoromethylthiolation and Trifluoromethylselenolation of (Hetero)Aromatic Amines Catalyzed by Copper *Chem. Eur. J.* **2016**, *22*, 79–82. (e) Nikolaienko, P.; Rueping, M. Trifluoromethylselenolation of aryldiazonium salts: a mild and convenient copper-catalyzed procedure for the introduction of the SeCF₃ group *Chem. Eur. J.* **2016**, *22*, 2620–2623. (f) Dong, T.; He, J.; Li, Z.-H.; Zhang, C.-P. Catalyst- and additive-free trifluoromethylselenolation with [Me₄N][SeCF₃]. *ACS Sustainable Chem. Eng.* **2018**, *6*, 1327–1335. (g) Ghiazza, C.; Debrauwer, V.; Monnereau, C.; Khrouz, L.; Médebielle, M.; Billard, T.; Tlili, A. Visible-light-mediated metal-free synthesis of trifluoromethylselenolated arenes, *Angew. Chem. Int. Ed.* **2018**, *57*, 11781-11785.

⁶ Chen, C.; Ouyang, L.; Lin, Q.; Liu, Y.; Hou, C.; Yuan, Y.; Weng, Z. Synthesis of Cu^I trifluoromethylselenates for trifluoromethylselenolation of aryl and alkyl Halides. *Chem. Eur. J.* **2014**, *20*, 657–661.

⁷ Aufiero, M.; Sperger, T.; Tsang, A. S.-K.; Schoenebeck, F. Highly efficient C-SeCF₃ coupling of aryl iodides enabled by an air-stable dinuclear Pd(I) catalyst. *Angew. Chem. Int. Ed.* **2015**, *54*, 10322-10326.

⁸ Dürr, A. B.; Fisher, H. C.; Kalvet, I.; Truong, K.-N.; Schoenebeck, F. Divergent Reactivity of a Dinuclear (NHC)Nickel(I) Catalyst versus Nickel(0) Enables Chemoselective Trifluoromethylselenolation. *Angew. Chem. Int. Ed.* **2015**, *54*, 10322-10326.

⁹ Han, J.-B.; Dong, T.; Vivic, D. A.; Zhang, C.-P. Nickel-catalyzed trifluoromethylselenolation of aryl halides using the readily available [Me₄N][SeCF₃] salt. *Org. Lett.* **2017**, *19*, 3919–3922.

¹⁰ Krykun, S.; Durandetti, M. Nickel-Catalyzed Electrochemical Synthesis of (Hetero)Aryl Trifluoromethyl Selenides. *Eur. J. Org. Chem.* **2017**, *19*, 3919–3922.

¹¹ Derhamine, S. A.; Krachko, T.; Monteiro, N.; Pillet, G.; Schranck, J.; Tlili, A. Amgoune, A. Nickel-Catalyzed Mono-Selective α -Arylation of Acetone with Aryl Chlorides and Phenol Derivatives. *Angew. Chem. Int. Ed.* **2020**, *59*, 18948-18953.

¹² For the beneficial effect of nitrile on the stability and catalytic reactivity of Ni(0) species, see: (a) Yin, G.; Kalvet, I.; Englert, U.; Schoenebeck, F. Fundamental Studies and Development of Nickel-Catalyzed Trifluoromethylthiolation of Aryl Chlorides: Active Catalytic Species and Key Roles of Ligand and Traceless MeCN Additive Revealed. *J. Am. Chem. Soc.* **2015**, *137*, 4164–4172. (b) Ge, S.; Green, R. A.; Hartwig, J. F. Controlling First-Row Catalysts: Amination of Aryl and Heteroaryl Chlorides and Bromides with Primary Aliphatic Amines Catalyzed by a BINAP-Ligated Single-Component Ni(0) Complex Hartwig, *J. Am. Chem. Soc.* **2014**, *136*, 1617–1627. (c) Ge, S.; Hartwig, J. F. Nickel-Catalyzed Asymmetric α -Arylation and Heteroarylation of Ketones with Chloroarenes: Effect of Halide on Selectivity, Oxidation State, and Room-Temperature Reactions. *J. Am. Chem. Soc.* **2011**, *133*, 16330–16333. (d) Stolley, R. M.; Duong, H. A.; Thomas, D. R.; Louie, J. The Discovery of [Ni(NHC)RCN]₂ Species and Their Role as Cycloaddition Catalysts for the Formation of Pyridines. *J. Am. Chem. Soc.* **2011**, *133*, 16330–16333.

¹³ (a) Clevenger, A. L.; Stolley, R. M.; Aderibigbe, J.; Louie, J. Trends in the Usage of Bidentate Phosphines as Ligands in Nickel Catalysis. *Chem. Rev.* **2020**, *120*, 6124–6196 (b) Lavoie, C. M.; Stradiotto, M. Bisphosphines: A Prominent Ancillary Ligand Class for Application in Nickel-Catalyzed C–N Cross-Coupling. *ACS Catal.* **2018**, *8*, 7228–7250. (b) Yu, P.; Morandi, B.; Nickel-Catalyzed Cyanation of Aryl Chlorides and Triflates Using Butyronitrile: Merging Retrohydrocyanation with Cross-Coupling. *Angew. Chem. Int. Ed.* **2017**, *56*, 15693-15697.

¹⁴ Dürr, A. B.; Yin, G.; Kalvet, I.; Napoly, F.; Schoenebeck, F. Nickel-catalyzed trifluoromethylthiolation of Csp²–O bonds. *Chem. Sci.*, **2016**, *7*, 1076-1081.

-
- ¹⁵ Nicholas D. Staudaher, N. D.; Stolley, R. M.; Louie, J. Synthesis, mechanism of formation, and catalytic activity of Xantphos nickel π -complexes. *Chem. Commun.*, **2014**, *50*, 15577-15580.
- ¹⁶ CCDC-2260118 contains the supplementary crystallographic data for crystal structure of [(Xantphos)₂Ni(0)] complex. These data can be obtained free of charge from The Cambridge Crystallographic Data Centre via www.ccdc.cam.ac.uk/data_request/cif.
- ¹⁷ See Supporting Information for details
- ¹⁸ Yin, J.; Buchwald, S. L. Pd-Catalyzed Intermolecular Amidation of Aryl Halides: The Discovery that Xantphos Can Be Trans-Chelating in a Palladium Complex. *J. Am. Chem. Soc.* **2002**, *124*, 6043-6048.
- ¹⁹ For a rare example of XantphosNi(II) ArX, see: Standley, E. A.; Smith, S. J.; Müller, P.; Jamison, T. F, A Broadly Applicable Strategy for Entry into Homogeneous Nickel(0) Catalysts from Air-Stable Nickel(II) Complexes. *Organometallics*. **2014**, *33*, 2012-2018.
- ²⁰. (a) For Pt see: Kirij, N. V.; Tyrra, W.; Pantenburg, I.; Naumann, D.; Scherer, H.; Naumann, D.; Yagupolskii, Y. L. *J. Organomet. Chem.* **2006**, *691*, 2679–2685. (b) For Cu see ref 6. (c) No example of nickel SeCF₃ species have been reported, but the downfield shift and the region of the resonance signals are reminiscent of a related nickel(II)-SCF₃ previously reported, see: Zhang, C.-P.; Brennessel, W. W.; Vicic, D. A. *J. Fluorine. Chem.* **2012**, *140*, 112-115.
- ²¹ The formation of PhSeCF₃ is proposed to originate from aryl group exchange between Xantphos ligand and PhPhSeCF₃. For a related study, see: Lee, Y. H.; Morandi, B. Metathesis-active ligands enable a catalytic functional group metathesis between aryl chlorides and aryl iodides. *Nat. Chem.* **2018**, *10*, 1016–1022.
- ²² Diccianni, J. B.; Katigback, J.; Hu, C.; Dia, T. Mechanistic Characterization of (Xantphos)Ni(I)-Mediated Alkyl Bromide Activation: Oxidative Addition, Electron Transfer, or Halogen-Atom Abstraction. *J. Am. Chem. Soc.* **2019**, *141*, 1788–1796.
- ²³ Kalvet, I.; Guo, Q.; Tizzard, G. J.; Schoenebeck, F. When Weaker Can Be Tougher: The Role of Oxidation State (I) in P- vs N-Ligand-Derived Ni-Catalyzed Trifluoromethylthiolation of Aryl Halides. *ACS Catal.* **2017**, *7*, 2126–2132.
- ²⁴ Complex **III** was recently shown to be very efficient for the Ni(0)/Ni(II) catalyzed C-S bond formation see: (a) Oechsner, R. M.; Wagner, J. P.; Fleischer, I. Acetate Facilitated Nickel Catalyzed Coupling of Aryl Chlorides and Alkyl Thiols. *ACS Catal.* **2022**, *12*, 2233–2243. (b)

Oechsner, R. M.; Lindenmaier, I. H.; Fleischer, I. Nickel Catalyzed Cross-Coupling of Aryl and Alkenyl Triflates with Alkyl Thiols. *Org. Lett.* **2023**, *25*, 1655–1660.

²⁵ The bite angle might also contribute to ligand effectiveness as observed with DPEphos and DPPF. However, the catalytic performance doesn't align strictly with bite angle trends (Xantphos: 108° > Dppf: 99° > DPEPhos: 104°). This variation suggests the involvement of additional factors beyond just the angle. For bite angle values, see: *Chem. Soc. Rev.* 2009, 38, 1099-1118 Ref a mettre en forme